Journal of the Ceramic Society of Japan 114 [5] 380–385 (2006)

Paper

Volume Change of β-Spodumene s.s. Glass-Ceramics Due to Structural Relaxation

Akihiko SAKAMOTO and Shigeru YAMAMOTO

Technical Division, Nippon Electric Glass, 2–7–1, Seiran, Otsu-shi, Shiga 520–8639

構造緩和による β-スポジュメン固溶体結晶化ガラスの体積変化

坂本明彦・山本 茂

日本電気硝子(株), 520–8639 滋賀県大津市晴嵐 2–7–1

The high-temperature dimensional stability of β-spodumene solid solution (s.s.) glass-ceramics with different crystallinities was investigated. It was demonstrated that the glass-ceramics show volume change due to structural relaxation in the residual glass phase regardless of crystallinity, even in the specimen with a high crystallinity of 90 vol%. The volume change process was expressed by the Kohlrausch–Williams–Watts (KWW) function. In the specimens with lower crystallinity (52, 71 vol%), normal relaxation behavior like that of non-crystalline glasses was observed, with activation energies of 599 and 414 kJ/mol, respectively. In contrast, the specimen with a crystallinity of 90 vol% showed an anomalous relaxation behavior accompanied with a densification limit and lower activation energy (250 kJ/mol). This anomalous behavior was attributed to the inner friction caused by proximity of the crystal grains in the glass-ceramic, which may result in a blocking effect on the volume shrinkage. We predicted the long-term dimensional stability of a precision glass-ceramic capillary for fiber-optic devices, based on the relaxation data in the KWW function.

[Received December 21, 2005; Accepted April 19, 2006]

Key-words : *Glass-ceramic, Structural relaxation, Crystallinity, Densification limit, Inner friction, Dimensional stability*

1. Introduction

Li_2O–Al_2O_3–SiO_2 (LAS) glass-ceramics including the β-spodumene solid solution (s.s.): $Li_2OAl_2O_3nSiO_2$ ($4<n<10$) glass-ceramics have a long history starting from the first glass-ceramic invented by Stookey in 1959.[1] Since then, the LAS glass-ceramics have been extensively studied and applied in many industrial fields as low-expansion heat-resistant materials.[2)–4)] In addition to such traditional applications, the LAS glass-ceramics are recently also being applied in the field of information technology such as in fiber-optics and the flat-panel displays.[5),6)]

High-temperature dimensional stability is one of the most important properties of the LAS glass-ceramics in both traditional and modern applications. In general, we tend to think that glass-ceramics are stable under temperatures below the crystallization temperature. However, this is not the case when their long-term dimensional stability is considered. In such cases, the influence of the residual glass-phase on the stability should be taken into account in addition to the thermal stability of the crystalline phase. The residual glass-phase in glass-ceramics usually has a different chemical composition from that of the original glass before crystallization (precursor glass), unless the composition of the precipitated crystal is identical to that of the precursor glass. The dimensional stability of non-crystalline glasses has been widely investigated in correlation with the structural relaxation.[7)–9)] In contrast, there are few reports on the dimensional stability or structural relaxation of glass-ceramics, because, so far, the influence of the glass-phase on their properties has not been significantly noted. As for the β-quartz s.s.: $Li_2OAl_2O_3nSiO_2$ ($2<n<10$) glass-ceramics which contain nanometer-scale crystal grains, there are some reports describing that they show volume changes at high temperature due to the structural relaxation in the glass-phase.[10)–12)] However, in the case of β-spodumene s.s. glass-ceramics, which is another typical glass-ceramic in the LAS system, there are no detailed reports except for our earlier work describing the volume shrinkage of the LAS glass-ceramics at high temperatures.[11)] The crystal grain size of β-spodumene s.s. glass-ceramics, which is in the order of micrometer, is so much larger than that of β-quartz s.s. glass-ceramics that their relaxation behaviors might be very different. β-spodumene s.s. glass-ceramics possess high-temperature resistance and mechanical strength superior to those of β-quartz s.s. glass-ceramics, and hence tend to be used under severer conditions. Therefore, it is of significance to know the long-term dimensional stability of β-spodumene s.s. glass-ceramics at high temperature and predict their lifetime in practical use. In this paper, details of the volume change behavior in β-spodumene s.s. glass-ceramics are described, based on the experimental data for five types of β-spodumene s.s. glass-ceramics with different crystallinity and crystal grain size (**Fig. 1**). We also describe the long-term dimensional stability of a precision glass-ceramic capillary for fiber-optic devices, referring to the structural relaxation data.

2. Experimental

The crystallization conditions and characteristics of the β-spodumene s.s. glass-ceramics used in this study are summarized in **Table 1**. The composition of specimen A is $73SiO_2$, $12Al_2O_3$, $5Li_2O$, $2MgO$, $2TiO_2$, $1ZrO_2$, $2K_2O$, $3ZnO$ in molar percent. This glass-ceramic is used in fiber optic devices as the material for optical connecting components.[5),13)] Specimen A was prepared by crystallizing the precursor glass at 1190°C in an electric furnace followed by quenching to ambient temperature on a stainless-steel plate. This thermal history is equivalent to that in the actual production process of the glass-ceramic products for fiber optic devices. The crystalline phase consists of β-spodumene s.s. and small amount of gahnite ($ZnAl_2O_4$). The crystallinity and crystal grain size of specimen A were 52 vol% and 0.8 μm, respectively, which are also

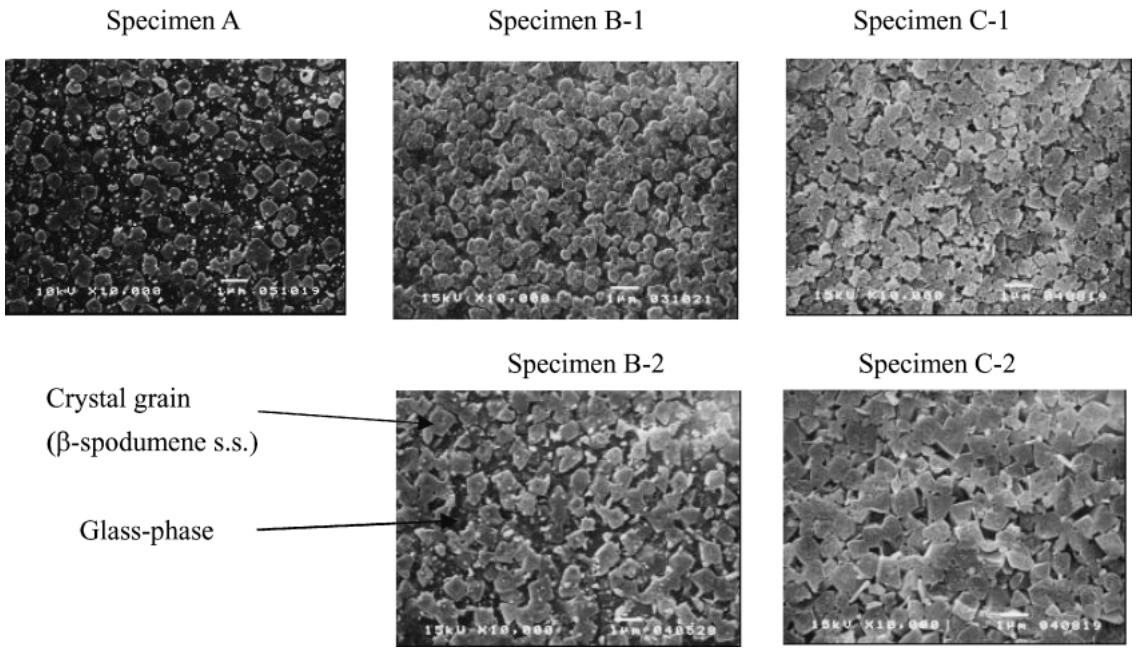

Fig. 1. SEM image of bulk structure of β-spodumene s.s. glass-ceramic specimens.

Table 1. Crystallization Conditions and Characteristics of β-Spodumene s.s. Glass-Ceramic Specimens

Specimen	A	B		C	
		B-1	B-2	C-1	C-2
Crystallization temp. /°C	1190	1000	1180	1150	1180
Crystallization time /h	1	8	8	1	8
Cooling	quench	rate-cooling		rate-cooling	
Crystallinity /vol%	52	71	72	90	90
Grain size /μm	0.8	0.5	1.0	0.7	1.1

equivalent to those of the actual products. Specimen B has the same chemical composition as specimen A, but was prepared by a different crystallization process with rate cooling. The crystallinity was approximately 70 vol% as shown in Table 1. Specimen C contains $72SiO_2$, $14Al_2O_3$, $9Li_2O$, $2TiO_2$, $1ZrO_2$, $0.5P_2O_5$, $0.5BaO$, $0.5Na_2O$, $0.5K_2O$. The crystalline phase was β-spodumene s.s., and the crystallinity was 90 vol%. For specimens B and C, two specimens with differnt grain size were also prepared by changing the crystallization conditions. They are expressed as specimens B-1, B-2 and C-1, C-2 as shown in Table 1 and Fig. 1. The crystal species and crystallinity of specimens B-2 and C-2 were identical to those of specimens B-1 and C-1, respectively.

To study the dimensional stability of the specimens, their density changes during high-temperature treatment were monitored. Specimens B and C were heat treated beforehand at prescribed temperatures and quenched to room temperature, in order to confer a certain fictive temperature. The pretreatment temperatures for specimens B and C were 900°C and 1000°C, respectively. As for specimen A, the fictive temperature was taken as 1190°C since it was prepared by quenching from that temperature. In the dimensional stability test, each specimen ($25 \times 24 \times 4$ mm) was heat treated at constant temperatures below the crystallization temperature in an electric furnace, then quenched on a stainless steel plate to room temperature. Density was measured by the Archimedes method with distilled water at ambient temperature. The density measurements were carried out four times in order to confirm the reproducibility of data. The experimental error range (3σ) in the measurement was within 0.0004 g cm^{-3}. The glass transition point (T_g) of the residual glass-phase in each glass-ceramic was determined from thermal expansion curves. We also simulated T_g using an international glass database system (INTERGLAD 6)[14] based on the estimated glass-phase composition. Crystallinity and crystal grain size were determined by scanning electron microscopy (SEM), with an image analyzing system. Figure 1 shows the micrographs of bulk structures of the specimens. Each specimen was subjected to SEM observation after etching with 2 mass% HF aqueous solution at 25°C for 2min. The reproducibility of the crystallinity and grain size was within $+/-3$ vol% and $+/-0.05$ μm, respectively. An X-ray diffractometer (RINT2000/PC, Rigaku) was used for the analysis of the crystalline phase. The intensity of the diffraction lines from the (201) plane of β-spodumene s.s. and (311) plane of gahnite was used to compare the amount of precipitated crystals.

3. Results

Figure 2 shows density changes in specimens A, B-1 and C-1 during the dimension stability tests. The observed density changes were confirmed to be due to the shrinkage of specimens, because the mass of each specimen was maintained constant throughout the experiments. The density changes of specimen C-1 for opposite direction of temperature shift was indicated in **Fig. 3**. The figure shows that the density change occurs reversibly. The reversibility of density change was observed in all other specimens as well. Furthermore, no specimen showed alterations in the characteristics of the crystalline phase, such as crystal species, crystallinity and lattice spacing, before and after the heat treatment. These results mean that the observed volume changes are due to the structural relaxation in the residual glass phase. The solid lines in Figs. 2 and 3 indicate fitting curves obtained from a relaxation function, the Kohlrausch–Williams–Watts (KWW) function, expressed by

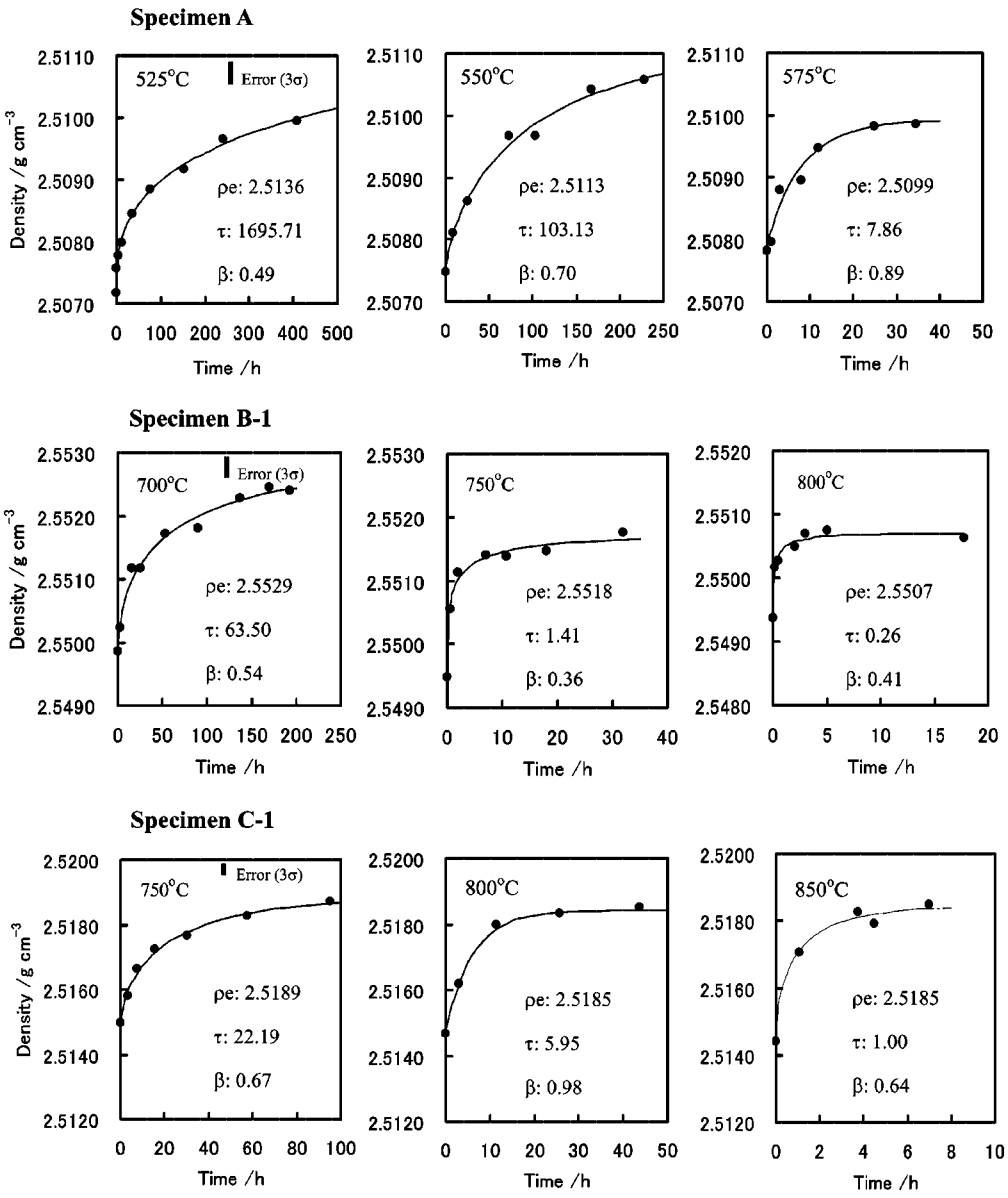

Fig. 2. Density changes in β-spodumene s.s. glass-ceramics during heat-treatment. Each dot represents average value of four measurements. Bars express typical error range (3σ) of the measurement.

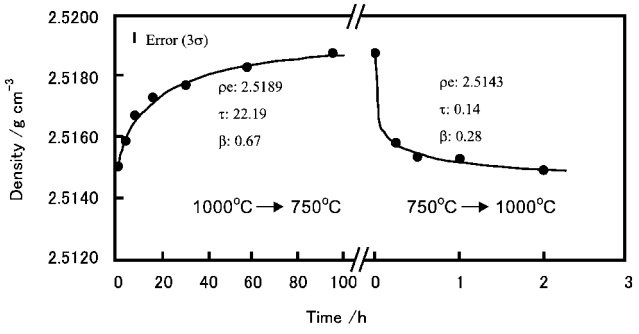

Fig. 3. Density change in specimen C-1 for both directions of temperature shift. Each dot represents average value of four measurements. Bar expresses typical error range (3σ) of the measurement.

$$\phi(t) = [\rho(t) - \rho_e]/[\rho_0 - \rho_e] = \exp[-(t/\tau)^{\beta}]. \quad (1)$$

Here, t represents the duration of heat-treatment, ρ_0 and ρ_e the initial and equilibrium densities, τ the relaxation time, and β a coefficient related to the number of relaxation modes ($0 < \beta < 1$). All experimental data were well approximated by the KWW function as shown in Figs. 2 and 3. The values of ρ_e, τ and β are indicated in each figure. The specimens with modified crystal grain size (specimens B-2 and C-2) also showed similar density changes that can be again expressed by the KWW function. As described above, it was confirmed that the volume of the β-spodumene s.s. glass-ceramics used in this study changes reversibly depending on the fictive temperature of the residual glass-phase, even in the specimen with a high crystallinity of 90 vol%.

4. Discussion

4.1 Viscosity of residual glass-phase

It is necessary to know the viscosity of the residual glass-phase of specimens in order to discuss their relaxation behavior. **Table 2** shows T_g and estimated compositions of the residual glass-phase. The simulated values of T_g are also indicated

Table 2. Estimated Composition and Glass Transition Point of Residual Glass-Phase

	Specimen A	Specimen B	Specimen C
SiO_2/mol%	79	83	56
Al_2O_3	12	9	30
Li_2O	2		
Na_2O			3
K_2O	6	8	4
MgO	1		
BaO			7
Total	100	100	100
Tg (measured)/°C	650	789	no data
Tg (simulated)/°C	615	785	818

besides the experimental values. The simulation of T_g was carried out by regression analysis using a glass database[14] based on the estimated composition of the glass-phase. Since the crystal species and crystallinity in specimen B-2 are identical to those of specimen B-1, the composition of their residual glass-phase should be the same. This is the case in specimens C-1 and C-2 as well. For the estimation of the glass phase compositions in specimens B and C, we assumed that all amounts of Li_2O, MgO and P_2O_5 crystallize as β-spodumene s.s. with the following molar composition: $(Li_{2-2w}Mg_wO)Al_2O_3xAlPO_4(n-2x)SiO_2$. Here, w is the ratio of the number of Mg atoms to that of Li atoms in the precursor glass, and x the molar ratio of $PO_{2.5}$ to $(Li_{2-2w}Mg_wO)$. Here, the value of n was set to be 7, the average value in its possible range $(4<n<10)$. ZrO_2 and ZnO were assumed to precipitate as $ZrTiO_4$ and $ZnAl_2O_4$, respectively, and the excessive amount of TiO_2 was considered to crystallize as $TiAl_2O_5$. $ZrTiO_4$ and $TiAl_2O_5$ act as the nuclei of β-spodumene s.s. For specimen A, the calculation was carried out assuming that the amount of precipitated β-spodumene s.s. is 0.7 times that in specimen B, based on the results of XRD and SEM analysis. As shown in the table, in specimens A and B, the calculated T_g was in substantial agreement with the experimental values. This suggests that the estimation of the glass-phase composition was satisfactory performed. For specimen C, the experimental value of T_g could not be obtained because the glass-phase fraction was too small to be detected. We use the simulated value instead in the following discussion.

4.2 Effect of structure on volume change

Figure 4 shows the Arrhenius plots of the relaxation time. The relaxation temperature markedly varied depending on the specimen. The temperature at a certain relaxation time (for instance, $\ln\tau=2$) decreased in the order of specimen A < B < C. In specimens B and C, no effect of crystal grain size on the relaxation time was observed, as shown in the figure. The order of relaxation temperature agrees with that of T_g listed in Table 2, indicating that the volume relaxation rate depends on T_g of the residual glass-phase. However, when we compare the relaxation time at T_g of the glass-phase, by extrapolating the Arrhenius plot, considerable discrepancy is found among the specimens, as shown in **Table 3**. In the case of non-crystalline glasses, it is known that the relaxation time at T_g can be approximated by $\ln\tau=-2$, as shown in the table.[15] Among the glass-ceramics used in this study, specimen B showed a closer relaxation time to those of non-crystalline glasses. The reason for the faster relaxation in specimen A than in specimen B can be attributed to its high fictive temperature (1190°C) and the resulting open structure of the glass-phase. In contrast, the relaxation time of specimen C was more than 30 times greater than those of non-crystalline glasses. This suggests that specimen C involves some effect that makes the volume change slower.

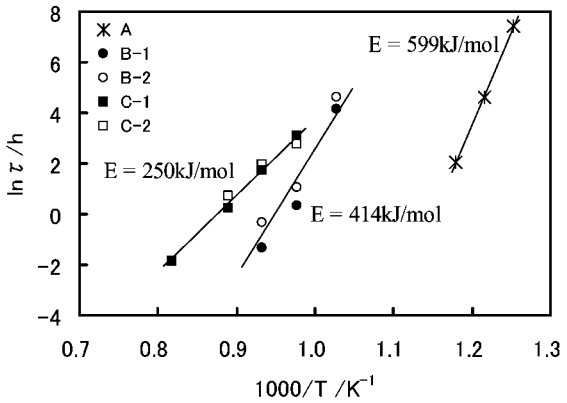

Fig. 4. Arrhenius plots of the relaxation time in β-spodumene s.s. glass-ceramics. Lines are drawn by the least squares method.

Table 3. Structural Relaxation Time at Glass Transition Point in Non-Crystalline Glasses and β-Spodumene s.s. Glass-Ceramics

	Non-crystalline glasses *			β-spodumen s.s. glass-ceramics		
	silica glass	borosilicate glass [a]	window glass [b]	A	B	C
Tg /°C	1152	486	524	650	789	818**
τ /h	0.089	0.117	0.111	0.005	0.497	3.669
lnτ /h	-2.4	-2.1	-2.2	-5.3	-0.7	1.3

* from Scherer [15]

[a] SiO_2: 64.4, B_2O_3: 22.3, Al_2O_3: 3.5, Na_2O: 3.0, K_2O: 5.5 (in mass%).

[b] SiO_2: 72.0, CaO: 6.7, MgO: 3.9, Al_2O_3: 1.7, Na_2O: 14.3, K_2O: 1.3 (in mass%).

** estimated value

Figure 5 shows the relationship between equilibrium density and temperature in specimens A, B and C. In a few cases, the density did not equilibrated within a practical observation time. In such cases, the equilibrium density was simulated based on the KWW function. In specimens A and B, as shown in the figure, the equilibrium density increased linearly with decreasing temperature in the temperature range below T_g of the glass-phase. This linear relation corresponds to the thermal expansion curve of the glass-phase below T_g. However, in the case of specimen C, a distinctive phenomenon was observed, in short, the equilibrium density was constant at temperatures below 850°C regardless of temperature and the crystal grain size. This means that the volume shrinkage of specimen C reached a "densification limit" when the fictive temperature of the glass-phase decreased to a certain criterion. This phenomenon can be attributed to the proximity of crystal grains due to the highly crystallized structure (Fig. 1, crystallinity: 90 vol%); namely, the crystal grains with increased proximity block the volume shrinkage of the glass-ceramic. Since such a densification limit was not observed in specimen A or B with similar grain sizes, it is clear that the grain size itself is not responsible for this phenomenon, but the proximity of crystal grains is. It is inferred from these results that the cause of the slower relaxation in specimen C is inner friction resulting from the proximity of crystal grains, which may decrease the rate of shrinkage. The activation energy of volume relaxation in specimens A and B were 599 and 414 kJ/mol, respectively, which are in fair agreement with those of non-crystalline silicate glasses.[7),16] However, the activation

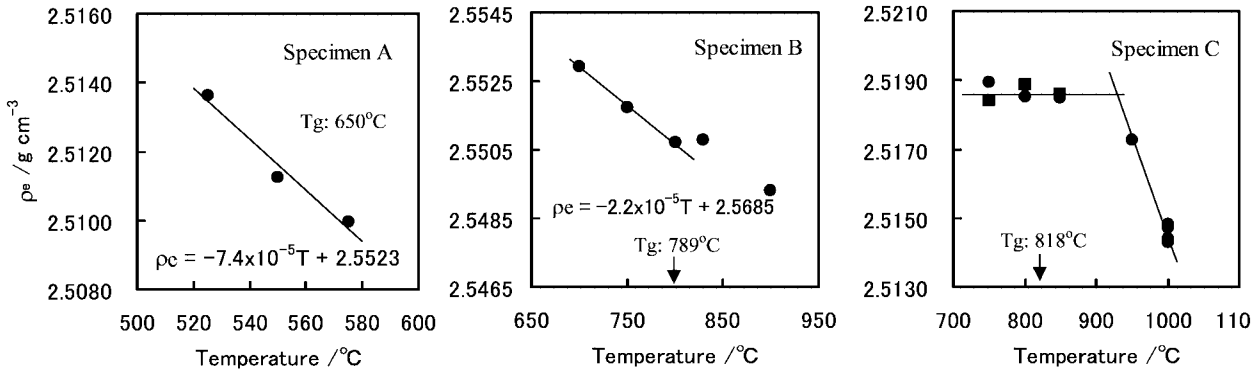

Fig. 5. Relationship between equilibrium density and temperature in β-spodumene s.s. glass-ceramics. Squares show the results for specimen C-2 with larger grain size. Lines for specimens A and B are drawn by the least-squares method. Lines for specimen C is drawn to show the tendencies.

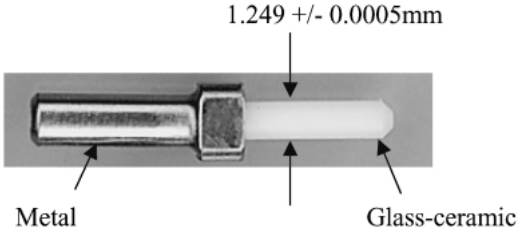

Fig. 6. Appearance of the glass-ceramic ferrule for optical fiber connectors.

energy of specimen C was much smaller (250 kJ/mol) than these values. This is also attributed to the friction between crystal grains, which may decrease temperature dependence of the rate of volume shrinkage. As described above, the volume change of β-spodumene s.s. glass-ceramics at high temperatures depends upon not only the viscosity of the glass-phase but also the crystalline-phase structure.

4.3 Simulation of long-term dimensional stability

Although the volume change of the β-spodumene s.s. glass-ceramics is influenced by their crystalline-phase structure, its time-dependent behavior can be well approximated by the KWW function. Therefore, it is possible to predict the long-term dimensional stability of the glass-ceramic using the KWW function. In the following, we discuss the diameter change of a precision glass-ceramic capillary used for the ferrules of optical fiber connectors (**Fig. 6**),[5),17)-19)] which has the same chemical composition and bulk structure as specimen A. The fictive temperature of the glass-ceramic capillary is considered to be identical to that of specimen A because of their equivalent thermal history. For low-loss optical connection, the accuracy of the ferrule diameter must be within a range of $+/-0.5\,\mu$m even if the ferrule is exposed to high temperatures.[20)-22)] We simulated the diameter change of a glass-ceramic ferrule with a diameter of 1.25 mm, based on the relaxation data for specimen A. The diameter change can be calculated from the initial density ρ_0, equilibrium density ρ_e, relaxation time τ and the constant β in the KWW function. Now, ρ_0 is known, and τ can be determined from the Arrhenius plot at arbitrary temperature. It is known that β converges on 0.4 to 0.6 near the glass transition point.[23)] This was confirmed in this study as well; therefore, we set the value of β to be 0.5. For ρ_e, a linear relation $\rho_e = -7.4\times10^{-5}\,T + 2.5523$ (T: temperature in centigrade), is derived from Fig. 5 for specimen A, so that we can determine the value of ρ_e using this relation. The values of these terms used for the calculation are listed in **Table 4** for three different temperatures. **Figure 7** shows the simulation results of the diameter change of the glass-ceramic ferrule exposed to high temperatures. At 550°C, the diameter shrinks by 0.5 μm after 100 h, and then it becomes constant because the relaxation reaches equilibrium. However, at 500°C, although the initial volume change is slower than that at 550°C, the diameter continuously decreases and the amount of shrinkage reaches more than 1.2 μm, because the relaxation does not reach equilibrium within the calculation period. At 450°C, the shrinkage remains within 0.4 μm even after 1000000 h (more than 100 years) because of a very slow relaxation. These data indicate that the dimensional change depends on both the relaxation rate and the difference between the actual temperature and the fictive temperature of the glass-ceramic. Since the allowed accuracy for

Table 4. Factors in the KWW Function Used in Calculation of Diameter Change in the Glass-Ceramic Ferrule

Temp. /°C	ρ_0 /g cm^{-3}	ρ_e /g cm^{-3}	τ /h	β
450	2.5075	2.5190	17.3 x 10^6	0.5
500	2.5075	2.5153	27.3 x 10^3	0.5
550	2.5075	2.5109	103.1	0.5

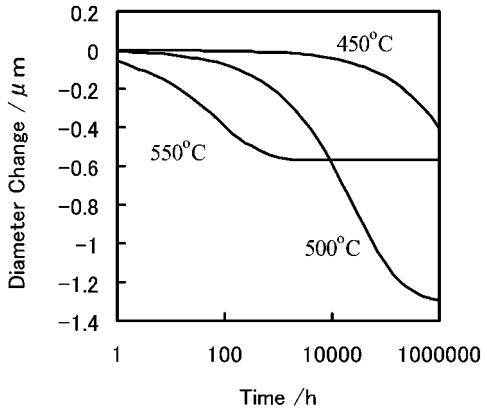

Fig. 7. Diameter change in the glass-ceramic ferrule at high temperatures.

the ferrule diameter is $+/-0.5\ \mu m$, we can say that the glass-ceramic ferrule has a sufficient dimensional stability at temperatures below 450°C for sufficiently long periods of time. If the glass-ceramic ferrule has a lower fictive temperature, the rate of diameter change will be slower.

5. Conclusion

The high-temperature dimensional stability of β-spodumene s.s. glass-ceramics was investigated. We demonstrated that the glass-ceramics show reversible volume change due to the structural relaxation in the residual glass-phase, even in a highly crystallized specimen (crystallinity: 90 vol%). The relaxation behavior in the specimens with lower crystallinity (<70 vol%) was similar to that of non-crystalline glasses, while it is distinct in the highly crystallized specimen, that is, it showed a densification limit and lower activation energy. These phenomena were attributed to a blocking effect due to the proximity of the precipitated crystal grains. The volume change process in all specimens was well expressed by the KWW function regardless of the crystallinity. We predicted long-term dimensional change of a glass-ceramic ferrule for optical fiber connectors, on the basis of relaxation data obtained from the KWW function. This study will be valuable for understanding high-temperature stability of the β-spodumene s.s. glass-ceramics.

References

1) Stookey, S. D., *Ind. Eng. Chem.*, Vol. 51, pp. 805–808 (1959).
2) Pannhorst, W., "Low Thermal Expansion Glass Ceramics," Ed. by Bach, H., Springer (1995) pp. 4–6.
3) Tashiro, M. and Wada, M., Proc. 6th Int. Cong. Glass, "Advan. Glass Technolo.," Plenum Press (1963) pp. 18–19.
4) Tashiro, M., *Glass Ind.*, Vol. 47, pp. 366–373 (1966).
5) Sakamoto, A. and Yamamoto, S., *J. Mater. Sci.*, Vol. 38, pp. 2305–2310 (2003).
6) Endo, S., Murata, M. and Ushiki, T., JP1, 901, 174.
7) Kato, Y., Yamazaki, H. and Yamamoto, S., Proc. 20th Int. Cong. Glass (2004) O–10–047.
8) Rekhson, S. M. and Mazurin, O. V., *J. Am. Ceram. Soc.*, Vol. 57, pp. 327–328 (1974).
9) Mazurin, O. V., Rekhson, S. M. and Startsev, Y. K., *Sov. J. Glass. Phys. Chem.*, Vol. 1, pp. 412–416 (1975).
10) Sakamoto, A. and Yamamoto, S. Proc. 17th Univ. Conf. Glass Science (2005) pp. 17–17.
11) Sakamoto, A., Fujita, S. and Yamamoto, S., Proc. 20th Int. Cong. Glass (2004) O–07–055.
12) Dudek, R., Kristen, K. and Taplan, M., "Low Thermal Expansion Glass Ceramics," Ed. by Bach, H., Springer (1995) pp. 91–91.
13) Sakamoto, A., Asano, H., Wada, M., Yamamoto, S. and Nishii, J., *J. Ceram. Soc. Japan*, Vol. 111, pp. 640–644 (2003).
14) Iseda, T., Iwasa, Y., Yoshida, S. and Kawasaki, T., Proc. 20th Int. Cong. Glass (2004) P–07–029.
15) Scherer, G. W., "Relaxation in Glass and Composites," Krieger, Malabar (1992) pp. 143–143.
16) Fujita, S., Sakamoto, A. and Tomozawa, M., *J. Non-Cryst. Solids*, Vol. 330, pp. 252–258 (2003).
17) Mitachi, S., Nagase, R,. Takeuchi, Y. and Honda, R., *Glass Technol.*, Vol. 39, pp. 98–99 (1998).
18) Nagase, R., Takeuchi, Y. and Mitachi, S., *Electron. Letters*, Vol. 33, pp. 1243–1244 (1997).
19) Takeuchi, Y., Mitachi, S. and Nagase, R., *IEEE Photon. Technol. Letters*, Vol. 9, pp. 1502–1504 (1997).
20) Nagase, R., Sugita, E., Iwano, S., Kanayama, K. and Ando, Y., *IEEE. Photonics Technol. Letters*, Vol. 3, pp. 1045–1047 (1991).
21) Yanagi, S. and Nagase, R., Proc. IEICE General Conf. (2002) C–3–108 [in Japanese].
22) Nagase, R., Yanagi, S. and Asakawa, S., Proc. IEICE Soc. Conf. (2002) C–3–108 [in Japanese].
23) Torell, L. M., Borjesson, L. and Elmorth, M., *J. Phys.: Cond. Matter*, Vol. 2, pp. SA207–214 (1990).